Four free parameter empirical parametrization of glow discharge Langmuir probe data

A. A. Azooz
Department of Physics, College of Science, Mosul University, Mosul–Iraq

(Received 29 April 2008; accepted 10 August 2008; published online 3 October 2008)

For the purpose of developing a simple empirical model capable of producing the electron energy distribution function (EEDF) from Langmuir probe *I-V* characteristics, a four parameter empirical equation that fits most Langmuir probe experimental data is suggested. The four free fitting parameters are related to the main plasma properties. These properties include the ion and electron saturation currents and the plasma electron temperature. This equation can be readily differentiated twice to give the EEDF according to the Druyvesteyn formula. Furthermore, a MATLAB platform based computer code based on this model yielding results for the plasma potential and all plasma parameters mentioned above is presented. The information given below can be used to write other computer codes for the same purpose in any other programming language. © *2008 American Institute of Physics.* [DOI: 10.1063/1.2976755]

I. INTRODUCTION

Langmuir probes have been used for almost a century now as powerful plasma diagnostics tool.[1–5] Proper probe design coupled with careful data analysis techniques can, in principle, at least give all the information concerning plasma parameters. This information include the plasma ion density, the plasma electron density, the plasma potential, the plasma electron temperature, and the plasma electron energy distribution function (EEDF). The latter is of particular importance because it is the key for most other plasma parameters. The basic trick used for obtaining the EEDF is the exploitation of the Druyvesteyn formula[1]

$$F(E) = \frac{(8\ \mathrm{mV})^{1/2}}{Ae^{3/2}n}\frac{d^2I}{dV^2}, \qquad (1)$$

where m is the mass of the electron, e is the charge of the electron, A is the probe area, n is the electron number density, I is the probe current, and V is the probe voltage.

According to Eq. (1), one can, in principle, at least obtain the EEDF from the evaluation of the second derivative of the single Langmuir probe *I-V* characteristics curve. Simple as it may look, yet, the task of finding the second derivative of experimental data is not at all that straightforward. Several techniques have been developed for such purpose. These techniques fall into three main categories. The first category involves applying the Langmuir probe current signal to an analog double differentiating circuit.[6,7] The second category involves performing numerical differentiation after performing one kind or another of data smoothing.[8] The third method makes the use of a differentiating ac signal superimposed on the dc probe bias voltage.[9,10] The problems associated with the first kind of methods are mainly related to electronic noise and analog circuit time resolution. Numerical differentiation, on the other hand, can produce acceptable results only when the number of adjacent data points is large enough such that segment by segment polynomial fits are carried out with at least ten data points per segment. This condition can only be satisfied when very fast computer data acquisition systems are used. Even then, smoothing of data fluctuations may considerably modify the actual data. Methods of evaluating the second derivative through the application of a small ac differentiating signal need to be coupled with knowledge of the instrument convolution function.[11]

The situation is different for Langmuir double probe. Although the EEDF cannot be obtained using double probes, experimental *I-V* curves of such symmetric probes are theoretically described by tangent hyperbolic functions of the type.[12]

$$I = I_0 \tanh\left[\frac{e(V - V_{ff})}{2kT}\right], \qquad (2)$$

where I_0 is the ion saturation current and V_{ff}, is the difference between the floating potentials of the plasmas surrounding each of the two probes.

Among the hypotheses leading to Eq. (2) is the equivalence between ion and electron densities. Three free parameter fitting of double probe experimental data can directly lead to ion density, plasma potential, and electron temperature. Some attempts of using four free parameter fittings of single Langmuir probe data have been cited in literature.[13]

The single probe is, in fact, a special extreme type of double probe where one of the probes (the anode) has a very large area.[2,14] The aim of this work is to suggest and test an empirical equation that can simultaneously describe all regions of the single Langmuir probe *I-V* characteristics. Such equation, when fitted to experimental data, and analytically differentiated twice, can easily give plasma parameters in accordance with Eq. (1).

II. THE MODEL

In order to reach a reasonable empirical equation that can describe the single Langmuir probe *I-V* characteristics, one has to try to make a starting guess on what mathematical form such equation may take for a typical *I-V* characteristics. Irrespective of what they physically represent, both single and double probe characteristics contain two saturation regions. From mathematical point of view, such regions are well described by the tangent hyperbolic function. This is indeed true for the double probe based on theoretical bases. However, the situation with single probe is quite different. The upper saturation is a result of electron current while the lower is a direct result of ion saturation. The latter is usually few orders of magnitude lower than the former. This behavior can be mathematically represented by the application of an exponential transformation to a tangent hyperbolic function. We may thus write

$$I = \exp\left[a_1 \tanh\left(\frac{V+a_2}{a_3}\right)\right] + a_4. \tag{3}$$

These four free fitting parameters are related to plasma properties in the following manner.

(1) Irrespective of a_2 and a_3, and as V becomes highly negative, the tangent hyperbolic term will reach the limiting value of -1. Thus, the ion saturation current will become

$$I_{\mathrm{is}} = e^{-a_1} + a_4. \tag{4}$$

(2) At sufficiently large positive values of V, the limiting value of the tangent hyperbolic term will practically equal to $+1$. This will give the electron saturation current

$$I_{es} = e^{a_1} + a_4. \tag{5}$$

(3) Solving Eq. (3) for $I=0$ will yield the probe floating potential

$$V_f = a_3 \tanh^{-1}[\ln(-a_4)/a_1] - a_2. \tag{6}$$

Although the value plasma electron temperature derived from the EEDF using the fitted characteristics is more or less affected by all four fitting parameters, it must be pointed out, however, that extensive simulation work has indicated that this temperature is more strongly influenced by the fitted value of a_3 than to the other three fitting parameters. This is because a_3 plays a major role in defining the steepness of the increase in the probe current in the region below the plasma potential.

Let us consider the following arbitrary but some how realistic set of the four parameters $a_1=3, a_2=2, a_3=2,3,4,5, a_4=-1$. (Keeping the values of all other three free parameter constant, the value of a_3 is changed between 2 and 5). The simulated Langmuir probe *I-V* characteristics for the above set of free parameters are plotted in Fig. 1.

To examine the suitability of the suggested empirical equation further, one needs to remember that any representative empirical *I-V* equation of a single Langmuir probe must reflect the existence of the plasma potential. V_P. At probe voltage equals to the plasma potential, the second derivative of the probe current with respect to the probe voltage $d^2I/dV^2=0$ which represents the inflection point on the *I-V* curve. Differentiating Eq. (3) twice and arranging the terms gives

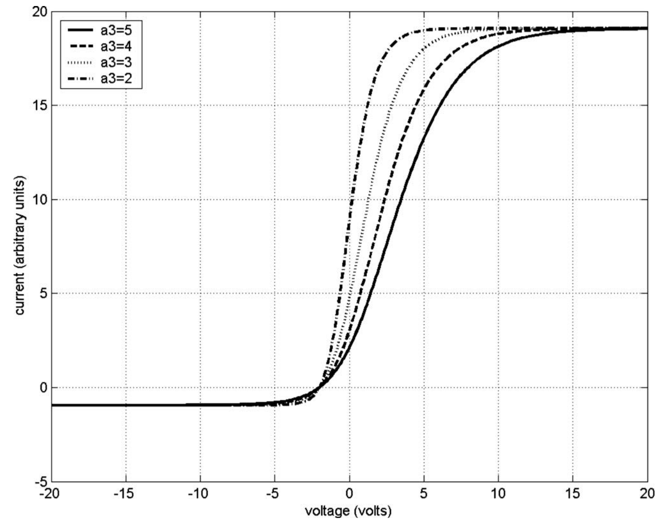

FIG. 1. Simulated *I-V* probe characteristics.

$$\frac{d^2I}{dV^2} = a_1\left[\tanh^2\left(\frac{V+a_2}{a_3}\right)\right]\left[2\tanh\left(\frac{V+a_2}{a_3}\right) - a_1 + \frac{a_1}{a_3^2}\tanh^2\left(\frac{V+a_2}{a_3}\right)\right]\exp\left[a_1\tanh\left(\frac{V+a_2}{a_3}\right)\right]. \tag{7}$$

The second derivatives obtained from Eq. (7) are plotted in Fig. 2 for the four sets of parameters above.

Values of the plasma potential obtained from the points of intersections of the graphs in Fig. 2 are -0.20, 0.67, 1.50, and 2.50 for the corresponding values of $a_3=2,3,4$, and 5, respectively.

These results are obtained graphically from Fig. 2. However, they represent analytical solutions of Eq. (7) at $d^2I/dV^2=0$ which gives

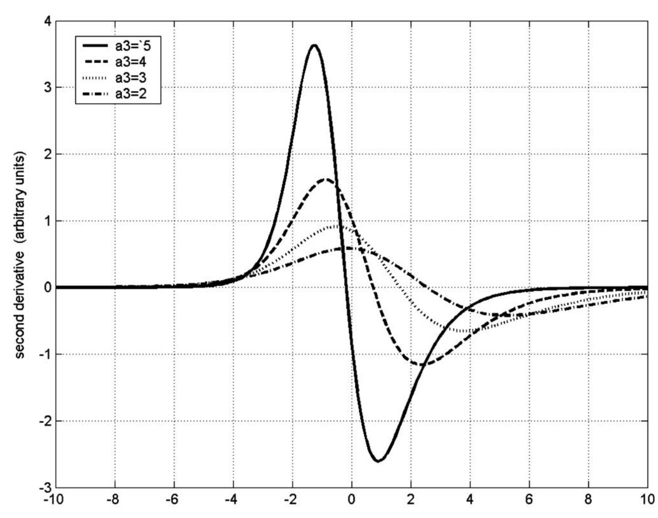

FIG. 2. Plots of the second derivative of the probe current against the probe voltage for the simulated *I-V* characteristics in Fig. 1.

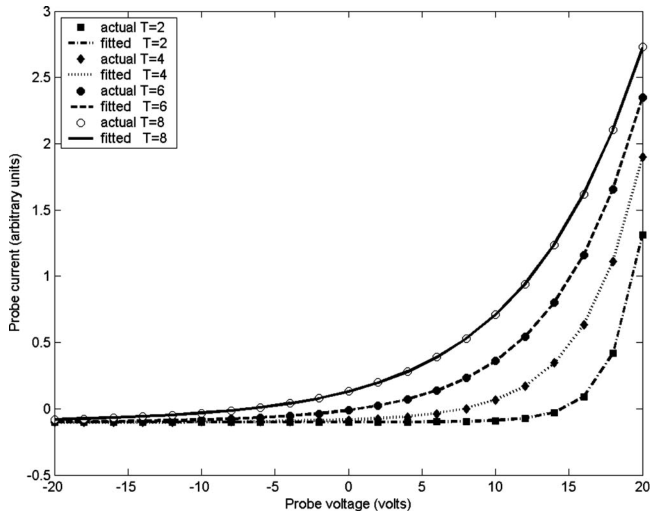

FIG. 3. Comparison of Maxwellian distribution *I-V* curves to model fittings at temperature values of 2, 4, 6, and 8 eV.

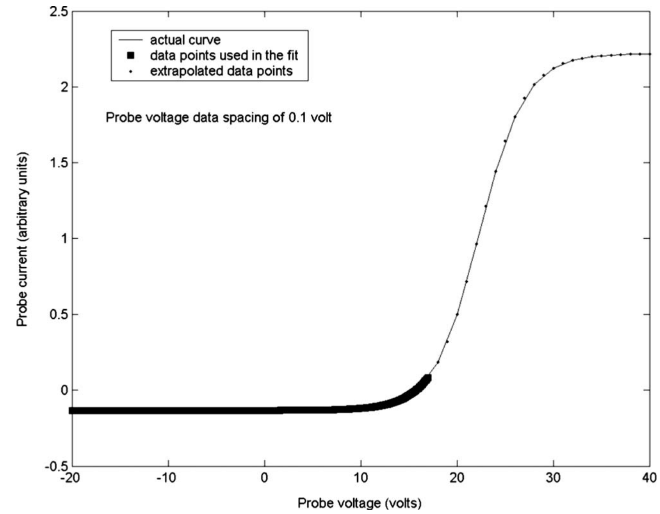

FIG. 4. Results of extrapolation to predict the model ability to cover the unmeasured part of the *I-V* characteristics for data spacing of 0.1 V.

$$V_p = a_3 \tanh^{-1}\left[\frac{(1+a_1^2)^{1/2}-1}{a_1}\right] - a_2. \quad (8)$$

The model assumes no specific experimental situations as far as the geometrical or effective probe area are concerned. The probe electron collection, for example, can be hindered when the probe is under the action of a magnetic field. Ion collection, on the other hand, is not so much affected. The model treats electron and ion currents simultaneously and adjusts itself according to the experimental data. Simulation tests representing such situation indicated no significant effect of changing the electron current on the deduced values of the plasma electron temperature or plasma potential. It must be mentioned, however, that no collision effects are considered in these simulations. Furthermore, overall random data fluctuations of up to 10% produced about 1% fluctuations on a_2, and a_4, and 5% on a_1, and a_3. The latter is the dominant parameter affecting the deduced temperature.

Three more tests are carried out to establish the ability of the model to handle situations generally encountered in the plasma physic Langmuir probe experiments. The first test is the assessment of the model's ability to reproduce the *I-V* characteristics associated with a well known Maxwellian electron energy distribution function. According to the Langmuir theory,[2] as the probe bias (V) becomes increasingly negative with respect to the plasma potential (V_p), only those electrons with increasing energies are collected. Assuming the electron energy distribution to be Maxwellian, the current drawn by the probe over this region, I_e, can be written[2]

$$I_e = I_0 \exp\left[\frac{e(V-V_p)}{kT_e}\right] \quad \text{with} \quad I_0 = n_e eA\left(\frac{kT_e}{2\pi m_e}\right)^{1/2}, \quad (9)$$

where I_e is the probe current after subtracting the ion saturation current, n_e is the plasma electron density, and A is the probe area. Probe characteristics of Eq. (9) are plotted for four temperatures values of $T=2,4,6$, and 8 eV on Fig. 3, using the normalized current $I_0=T^{1/2}$. An arbitrary 0.1 units of negative ion current is added to the electron current data of Eq. (9) in order to get the simulation more close to reality. (This has no effect on the fit except changing the fitted value of a_4.) These generated data are fitted with Eq. (3). The fits are shown on the same figure. No significant differences are found between the fits and the data. Furthermore, the model gave the correct EEDF and the associated Maxwellian temperature values for all cases.

The second and third tests are related to experimental situations where there are problems associated with obtaining the electron saturation part of the probe *I-V* characteristics. Two types of such situations are common. The first is where the positive applied voltage is lower than that needed to reach electron saturation. Simulations using generated *I-V* curves representing such situation are carried out. Different portions of data points below the electron saturation regions are selected and used in the model fitting program. The fit is then extrapolated to cover the entire range of the data. It has been found out that the model produces the correct extrapolation, for all situations when the fitted data cover points between ion saturation and the plasma potential. This condition can be relaxed further when the data points are closely spaced. Probe voltage data spacing of 0.1 V produced correct extrapolations even when the actual data used in the fitting were confined between the ion saturation region and the floating potential. This can be seen in Fig. 4. However, false extrapolations are obtained when the first condition was not satisfied and the data spacing was increased to one volt. This is demonstrated in Fig. 5.

Simulation tests of electron saturation fluctuations are also carried out. These test involved adding random fluctuations to the probe current in the region starting from the position where the probe current reaches 80% of the electron saturation value. Maximum current fluctuations between 10% and 100% of the saturation value are added. The fit was repeated twenty times for each case. Due to the random nature of the fluctuations superimposed on the actual curve, the fitted parameters obtained from different runs are not equal. Figure 6 shows the results of only five such repeated runs for

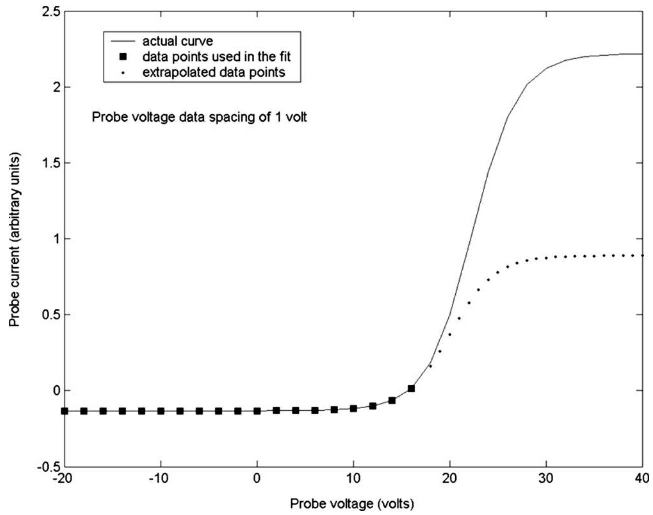

FIG. 5. Results of extrapolation demonstrating the model inability to correctly predict the unmeasured part of the *I-V* characteristics for data spacing of 1 V.

figure clarity purpose. The two model fitting parameters found to be susceptible to such fluctuations are a_1 and a_3. While 10% fluctuation produced only about 5% errors on those two parameters, these errors increased to about 30% and 65% when the fluctuations are 20% and 50%, respectively. This analysis suggests that in cases where there are high electron saturation current fluctuations, it may be more useful not to include the fluctuating region of the data in the fit. Instead, one can use the model extrapolation in that region to predict the electron saturation current provided that more accurate and reasonably spaced data are available else where on the *I-V* curves.

III. THE SOFTWARE

A software package in (MATLAB) language capable of carrying out all the Langmuir probe data analysis is written by the author. The software can be freely downloaded as a ZIP file from the MATLAB file exchange library.[15] The inputs to this software are the probe *I-V* data and starting guess

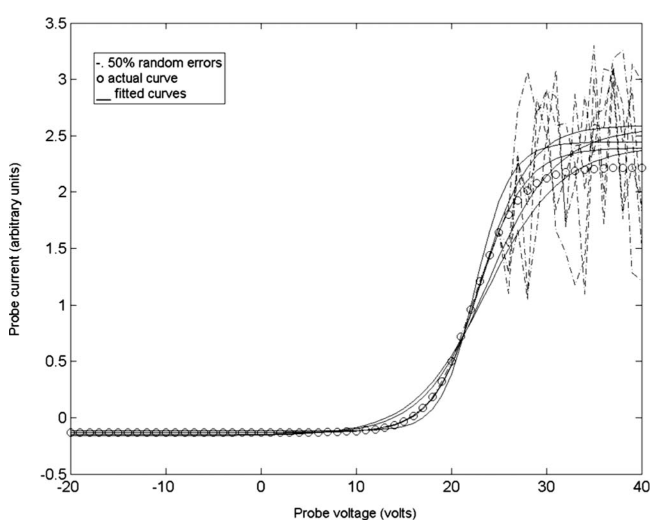

FIG. 6. Simulation representing 50% electron saturation current fluctuations

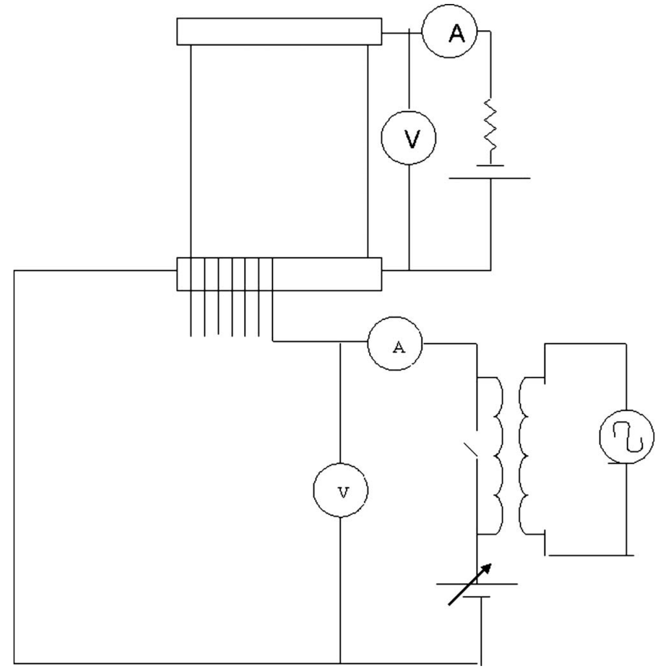

FIG. 7. Circuit diagram of experimental setup.

values of the four fitting parameters. The program running is not so critical to those starting values. Outputs of the program are the saturation electron current, the saturation ion current, the plasma potential, the plasma electron temperature, and the normalized EEDF. The EEDF produced is normalized such that the area under the curve is equal to one. Full instructions on how to run the program intended for users who are unfamiliar with MATLAB is included in the ZIP file as a PDF file. This will eliminate the need to have any prior knowledge of MATLAB programming. The only prerequisite to run the software is to have any version of MATLAB program installed on the PC. No special case dependent modifications to the program are needed as far as probe voltage or current ranges are concerned. However, the current measuring units, the electronic charge, and the effective probe area need to be externally substituted in order to calculate the electron number density from the normalized EEDF. As far as the effective probe area is concerned, the value used is geometry and magnetic field dependent and has to be treated on case by case bases.

IV. EXPERIMENTAL TEST

In an attempt to asses the applicability of the suggested fitting method, the radial dependence of the EEDF at the anode dark space region of air glow discharge is studied. Results obtained using the fitting method, and the ac differentiating signal methods are compared. The experimental setup is shown in Fig. 7. It consists of a 10 cm in length and 5 cm in diameter glass tube. The two ends of the tube are fitted with two flat disk shaped aluminum electrodes. Nine 0.2 mm in diameter insulated tungsten wires are introduce through nine boreholes drilled through one of the electrodes (the anode). The holes are distributed along the anode radius with equal center to center spacing of 2.6 mm epoxy resin is used for both insulation and filling the space between the

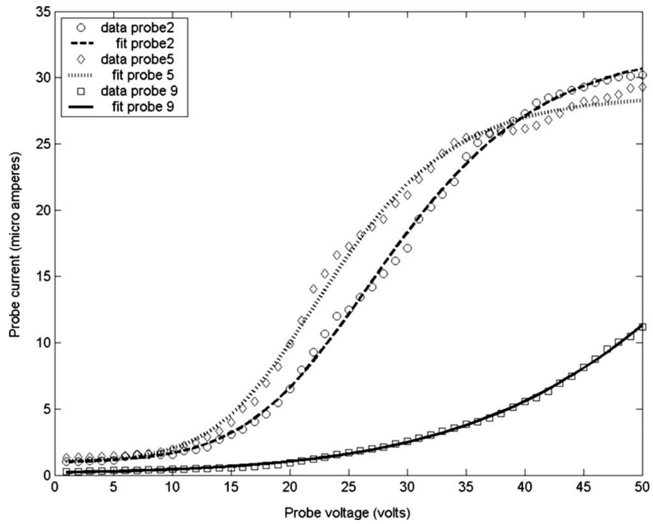

FIG. 8. Experimental and fitted *I-V* characteristics for three probes.

wires and the surrounding borehole. The face side of the anode facing the discharge is fine machine shaped and polished to ensure that the probes circular surfaces and the anode surface are equally flat. This will allow the probes to attract only electrons from negative anode sheet. The discharge is initiated by a HT power supply which has a 1 MΩ internal resistance. The Langmuir *I-V* probe measurements with and with out a 1000 Hz ac differentiating signal super imposed on the dc bias are measured by hand for the dc voltage range between −10 to 50 V in equal steps of 1 V.

Measurements are carried out using air discharge plasma at pressure of 2.5 Pa. Probe dc characteristics for three of the probes are shown in Fig. 8. Characteristics for other probes are much similar to probes 2 and 5. The current scale of probe 9 is lower than those obtained for other probes. This probe is very close to the glass discharge vessel where wall effects are dominant. Evaluation of the second differential d^2I/dV^2, plasma potential V_p, the EEDF, and thus the plasma electron temperature T_e are carried out using both the fitting method and ac differentiating signal data. Typical plot of d^2I/dV^2 and the EEDF using both methods for one of the probes are shown in Fig. 9.

It can be said that there is an acceptable agreement between values of the plasma potential and the general shape of the EEDF obtained using the two methods. Part of the discrepancies between the two may be associated with some of the limitations associated with ac differentiation. One of these limitations is connected to the experimental difficulty of measuring very small differences in probe current for the ac on and ac off cases. This is particularly true at higher probe dc probe biases that correspond to the higher electron energy tail of the EEDF. A second limitation associated with ac differentiation is the effect of instrument convolution function. The latter limitation results from the fact that the ac differentiator does not directly measures $I''(V)=d^2I/dV^2$, but, instead, it gives a convolution $J''(V)$ of $I''(V)$ with the instrumental function $\varphi(V-V')$.[11]

$$I''(V) = \int J''(V) \,.\, \varphi(V - V')dV' . \tag{10}$$

It is our purpose here to only demonstrate that the suggested analytical fitting equation and the following analytical differentiation produce results that are roughly not far from those obtained by an alternative method. EEDFs obtained

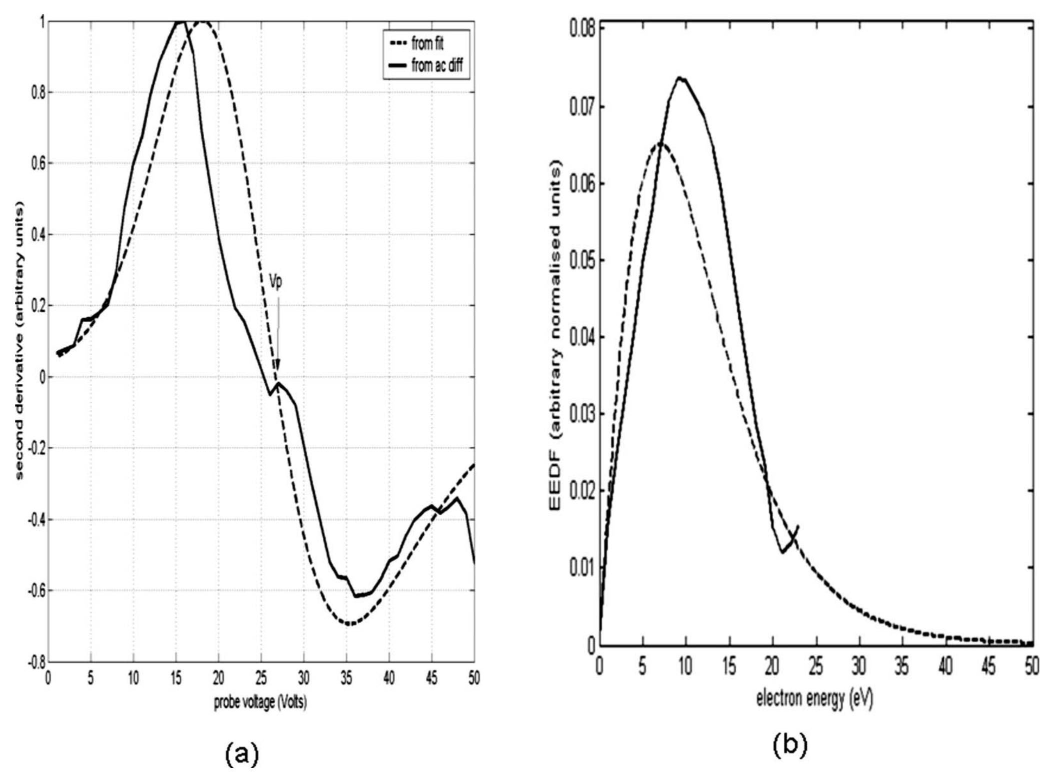

FIG. 9. (a) Experimental second differentials, (b) EEDF obtained, using ac differentiator (solid line) and fitting method (dashed line).

TABLE I. Results of plasma potential and temperature using fitting and ac differentiator methods.

R (mm)	0.0	4.0	8.0	12.0	16.0	20.0	24.0
V_{p1}	38.1	24.0	24.0	24.0	22.6	25.1	25.2
V_{p2}	38.7	24.0	25.0	24.2	24.4	25.6	26.5
T_{e1} (eV)	6.2	7.1	6.6	8.0	6.9	8.0	8.1
T_{e2} (eV)	4.2	7.7	5.7	8.2	7.0	8.3	8.3

using both methods are used to calculate the plasma potentials and the electron temperature at each probe position. Temperatures are calculated using

$$T_e = \frac{2}{3}\int Ef(E)dE, \quad (11)$$

where $f(E)$ is the EEDF and E is the energy. The units of both T_e and E are in electron volts.

Numerical trapezoidal rule integration is used for this purpose. Table I shows results obtained from using both methods. In this table, R represents the radial position of each probe measured from the anode center, V_{p1}, V_{p2}, T_1, and T_2 are the plasma potentials and electron temperatures measured by ac differentiation and fitting methods, respectively.

The overall average discrepancies between the two sets of values obtained are about 6%. The major discrepancy between the two sets of data is associated with the plasma electron temperatures obtained using the two methods is that at $R=0$. This may be related to the fact no instrument function convolution is applied in the ac differentiation procedure. Such convolution becomes more important at higher plasma potentials

V. CONCLUSIONS

The proposed empirical fitting equation of single Langmuir probe experimental data seems to provide a simple method for extracting the plasma parameters and the EEDF. No major discrepancies between results obtained using this method and the ac differentiation method. EEDF obtained using the fitting method extends to the higher energy tail region. The model can be used to obtain reasonable extrapolations to parts of the I-V curve not covered experimentally provided that data points of the measured part are narrowly spaced in voltage and do not have high current fluctuations. It must be pointed out, however, that although the model easily describes any type of distribution functions (Maxwellian and non-Maxwellian), it falls short from being able to produce EEDFs associated with plasma involving two groups of electrons with two distinct temperatures. (Langmuir probe characteristics with kinks). When the model is applied in such cases, the results obtained correspond only to an averaged EEDF with an averaged electron temperature. The model can be further expanded to handle such cases but that will certainly involve the use of more than four free fitting parameters.

ACKNOWLEDGMENTS

The author was indebted to the referee for his valuable suggestions concerning the tests on the model robustness in dealing with variety of situations encountered in Langmuir probe diagnostics.

[1] M. J. Druyvesteyn, Z. Phys. **64**, 781 (1930).
[2] J. D. Swift and M. J. R. Schwar, *Electrical Probes for Plasma Diagnostics* (Iliffe, London, 1970).
[3] F. F. Chen, R. H. Huddlestone, and S. L. Leonard, *Plasma Diagnostic Techniques* (Academic, New York, 1965).
[4] N. Hershkowitz, O. Auciello, and D. L. Flamm, *Plasma Diagnostics* (Academic, New York, 1989).
[5] P. C. Stangeby, in *The Interpretation of Plasma Probes for Fusion Experiments in Plasma Diagnostics*, edited by O. Auciello and D. L. Flamm (Academic, New York, 1989), Vol. 2.
[6] L. Kui-Xun, L. Xuan-Ying, C. Ling-Fei, Y. Chu-Ying, Y. Ruo-He, and Y. Yun-Peng, Chin. Phys. **12**, 198 (2003).
[7] A. Azooz and A. Hussein, Mu'tah Lil-Buhuth Wa Al-Dirasat **16**, 71 (2001).
[8] H. Andrei, V. Covlea, and E. Barna, Rom. Rep. Phys. **55**, 51 (2003).
[9] F. F. Elakshar, M. A. Hassouba, and A. A. Garamoon, Fiz. A **9**, 177 (2000).
[10] Yu. B. Pankrashkin and M. B. Shapochkin, Plasma Phys. Rep. **29**, 1056 (2003).
[11] Tsv. K. Popov, V. N. Tsaneva, N A. Stelmashenko, M. Dimitrova, M. G. Blamire, Z. H. Barber, and J. E. Evetts, Plasma Sources Sci. Technol. **14**, 184 (2005).
[12] G. Petraconi and H. S. Maciel Brazilian, Brazilian Journal of Physics **33**, 782 (2003).
[13] D. Desideri and G. Serianni, Rev. Sci. Instrum. **69**, 2354 (1998).
[14] H. Amemiya and S. Bhattacharjee, Proceedings of the 28th ICPIG, 15–20 July 2007, Prague, Czech Republic (unpublished).
[15] See http://www.mathworks.com/matlabcentral/fileexchange for MATLAB file exchange and search for Langmuir or Azooz will lead to the site where the code and full instructions on how to use it can be downloaded.